

Cosmic microwave background constraint on residual annihilations of relic particles

Patrick McDonald*

*Department of Astronomy, The Ohio State University, Columbus, Ohio 43210**and Department of Physics and Astronomy, University of Pennsylvania, Philadelphia, Pennsylvania 19104*Robert J. Scherrer[†] and Terry P. Walker[‡]*Department of Astronomy, The Ohio State University, Columbus, Ohio 43210**and Department of Physics, The Ohio State University, Columbus, Ohio 43210*

(Received 10 August 2000; published 14 December 2000)

Energy injected into the cosmic microwave background at redshifts $z \lesssim 10^6$ will distort its spectrum permanently. In this paper we discuss the distortion caused by annihilations of relic particles. We use the observational bounds on deviations from a Planck spectrum to constrain a combination of annihilation cross section, mass, and abundance. For particles with an (s -wave) annihilation cross section $\langle \sigma |v| \rangle \equiv \sigma_0$, the bound is $f(m_X/\text{MeV})^{-1}[(\sigma_0/6 \times 10^{-27} \text{ cm}^3 \text{ s}^{-1})(\Omega_{X\bar{X}} h^2)^2] < 0.2$, where m_X is the particle mass, $\Omega_{X\bar{X}}$ is the fraction of the critical density the particle and its antiparticle contribute if they survive to the present time, $h = H_0/100 \text{ km s}^{-1} \text{ Mpc}^{-1}$, H_0 is the Hubble constant, and f is the fraction of the annihilation energy that interacts electromagnetically. We also compute the less stringent limits for p -wave annihilation. We update other bounds on residual annihilations and compare them to our CMB bound.

DOI: 10.1103/PhysRevD.63.023001

PACS number(s): 98.70.Vc, 98.80.Cq, 98.80.Es, 98.80.Ft

I. INTRODUCTION

Newly proposed particles, especially dark matter candidates, must evade an ever growing array of empirical constraints, ranging from bounds obtained in terrestrial laboratory experiments (e.g., Ref. [1]), to limits on new cooling sources in stars in our galaxy [2], to constraints on the expansion rate of the universe during big bang nucleosynthesis (BBN), when the universe was only a few minutes old [3]. In this paper we add another constraint to the list, based on the effect of annihilations of relic particles on the cosmic microwave background (CMB).

The CMB energy spectrum provides a direct probe of the early Universe at redshifts as high as $z \sim 2 \times 10^6$. Below this redshift, distortions of the spectrum generally cannot be thermalized and are observable today. The FIRAS (Far Infrared Absolute Spectrophotometer) instrument on the COBE (Cosmic Background Explorer) satellite measured the spectrum and found it to have a Planck distribution to within a few hundredths of a percent [4]. This measurement places strong upper bounds on any energy injection into the CMB after the thermalization redshift (e.g., references [5,6]).

Decays of relic particles have been considered as a source of CMB distortions [7], but particle annihilations have not. Annihilations are typically ignored because the classic WIMP (weakly interacting massive particle) dark matter candidates have mass $m_X \gtrsim \text{GeV}$ and their annihilations “freeze out” at $T_F \sim m_X/20 \gtrsim 50 \text{ MeV}$ [8], long before the time when the CMB becomes vulnerable to distortion (at $T \approx 0.5 \text{ KeV}$). Freeze-out is defined as the time when annihilations cease to change significantly the number density of

the particle; however, annihilations continue eternally at some small rate and their products can distort the CMB spectrum if they interact electromagnetically.

The effects of residual annihilations have been considered in a few other contexts: Reno and Seckel [9], Hagelin, Parker, and Hankey [10], and Frieman, Kolb, and Turner [11] computed the effect of annihilation products on the primordial element abundances. Cline and Gao [12] and Gao, Stecker, and Cline [13] considered the possibility of observing directly the photons from annihilations at cosmological distances. Bergstrom and Snellman [14], Rudaz [15], and Rudaz and Stecker [16] discuss the detectability of a line source from annihilations to photons within the Milky Way halo. Jungman, Kamionkowski, and Griest [17] conclude that halo annihilations into particles other than photons probably cannot be used to place general constraints on particle candidates because of astrophysical uncertainties.

In this paper we compute the energy injected into the CMB by annihilating particles as a function of their mass and annihilation rate (i.e., the product of cross section and abundance squared). We derive constraints on the particle properties by comparison with the observed limits on chemical potential (μ) distortions, and Compton- γ distortions (Sec. II). We compare these constraints to similar constraints obtained from the production of deuterium by photodissociation of primordial helium (Sec. III A), and from the diffuse photon background produced after recombination by extragalactic annihilations (Sec. III B), and annihilations in the Milky Way halo (Sec. III C).

II. DISTORTIONS OF THE CMB ENERGY SPECTRUM

We consider first the effect of annihilation products on the CMB energy spectrum. The distortion of the spectrum takes place in two steps: first the high energy annihilation products rapidly dissipate their energy into the background photons

*Email address: mcdonald@astronomy.ohio-state.edu

†Email address: scherrer@pacific.mps.ohio-state.edu

‡Email address: twalker@pacific.mps.ohio-state.edu

and electrons, and then the low energy background evolves more slowly in an effort to restore the Planck spectrum. The permanence of distortions produced after $z \approx 10^6$ is simple to understand in the following way: A Planck spectrum with a given photon number density must have a specific energy density. For $z \lesssim 10^6$, photon nonconserving processes (double Compton scattering and bremsstrahlung) are inefficient in the background plasma. Therefore, if energy is injected into the CMB but not the correct number of photons, a Planck spectrum cannot be restored. We now discuss in more detail the form of the distortions produced in different redshift intervals.

Down to recombination at $z_{\text{rec}} \approx 1100$, photons with $E_\gamma \gtrsim 5$ KeV quickly cool and produce heated electrons by Compton scattering ($\gamma e \rightarrow \gamma e$) or pair production on ions ($\gamma N \rightarrow N e^+ e^-$) (all photons with $E_\gamma > 1$ KeV can cool if $z \gtrsim 3500$). The heated electrons quickly dissipate their energy by inverse Compton scattering on the huge number of CMB photons. This process produces a distorted spectrum with phase-space distribution

$$f(x, y) \approx f(x, 0) + y \frac{x e^x}{(e^x - 1)^2} \left[\frac{x}{\tanh(x/2)} - 4 \right], \quad (1)$$

where $f(x, 0) = 1/(e^x - 1)$ is the Planck distribution, $x = E/T$, and the Compton- y parameter is assumed to satisfy $y \ll 1$ [18]. In our case, where there is ample time for all of the input energy to be transferred to the CMB, the relation between y and the input energy can be found by integrating Eq. (1) to find the energy density as a function of y . The result is $4y = \delta\rho_\gamma/\rho_\gamma$, where $\delta\rho_\gamma$ is the injected energy and ρ_γ is the energy of the CMB photons (see Ref. [19] for a general review of CMB distortions or Ref. [18] for a more detailed discussion of the Compton- y distortion). Analysis of the COBE FIRAS data set gives $|y| < 1.5 \times 10^{-5}$ [4].

The Compton- y distortion will be preserved to the present time if it is produced after $z_C \approx 5.4 \times 10^4 \omega_B^{-1/2}$ (where $\omega_B \equiv \Omega_B h^2 / 0.02$), the redshift above which elastic Compton scattering would effectively redistribute energy between CMB photons, converting a Compton- y distorted spectrum into a Bose-Einstein spectrum with distribution

$$f(x, \mu) = \frac{1}{\exp(x + \mu) - 1}, \quad (2)$$

where μ is the chemical potential. Assuming the input number of photons is negligible, which will always be true in this paper, the chemical potential is $\mu = 1.4 \delta\rho_\gamma/\rho_\gamma$ [20]. The FIRAS limit on this type of distortion is $|\mu| < 9 \times 10^{-5}$ [4].

Equation (2) describes the equilibrium distribution for a fixed total number of photons and amount of energy. For $z \gtrsim z_{\text{DC}} \approx 2.1 \times 10^6 \omega_B^{-2/5}$, photons are produced effectively by double Compton scattering ($e\gamma \rightarrow e\gamma\gamma$) so a Planck spectrum ($\mu = 0$) can be restored for arbitrary energy input [20]. Production of photons by bremsstrahlung is already ineffective at $z \sim z_{\text{DC}}$ (for the observed baryon density).

To summarize: annihilations occurring at $z \gtrsim 2.1 \times 10^6$ will be unobservable, annihilations in the range 5.4×10^4

$\lesssim z \lesssim 2.1 \times 10^6$ will produce a Bose-Einstein spectrum with chemical potential μ , and annihilations in the range $1100 \lesssim z \lesssim 5.4 \times 10^4$ will produce a Compton- y distortion. Annihilations at $z < z_{\text{rec}}$ will not significantly affect the CMB energy spectrum, but can be observable in the diffuse photon background.

We now compute the fractional energy injection $\delta\rho_\gamma/\rho_\gamma$ (where ρ_γ is the energy density of the CMB) from annihilations of particle species X . We will assume throughout this paper that particle X and antiparticle \bar{X} are not identical (we discuss below how our final constraints are strengthened in the case where the particle is its own antiparticle). We also assume that $n_X \equiv n_{\bar{X}}$, where n_X ($n_{\bar{X}}$) is the number density of X (\bar{X}) (if there is a significant asymmetry the relic density of the less numerous particle will usually be negligibly small [21,22]). The energy produced per annihilating particle is

$$E_a \equiv f m_X, \quad (3)$$

where m_X is the mass of the particle and $f \leq 1$ is the mean fraction of the annihilation energy that interacts electromagnetically, and the rate of annihilations per unit volume is

$$\Gamma_a = \langle \sigma_a |v| \rangle n_X n_{\bar{X}}, \quad (4)$$

where $\langle \sigma_a |v| \rangle$ is the cross section. A useful parametrization for the cross section is $\langle \sigma_a |v| \rangle \equiv \sigma_0 (T/m_X)^n$, where $n = 0$ for s-wave annihilation (e.g., Dirac neutrinos) and $n = 1$ for p-wave annihilation (e.g., Majorana particles annihilating into much lighter fermions, see Ref. [23]). We integrate the energy injection rate from time t_1 to t_2 as follows:

$$\begin{aligned} \frac{\delta\rho_\gamma}{\rho_\gamma} &= \int_{t_1}^{t_2} \frac{\dot{\rho}_{\text{ann}}}{\rho_\gamma} dt = \int_{t_1}^{t_2} \frac{2E_a \Gamma_a}{\rho_{\gamma 0} (1+z)^4} dt \\ &= \frac{2E_a}{\rho_{\gamma 0}} \int_{t_1}^{t_2} \sigma_0 \left(\frac{T}{m_X} \right)^n n_{X0}^2 (1+z)^2 dt \\ &= \frac{4t_\star E_a \sigma_0 n_{X0}^2}{\rho_{\gamma 0}} \left(\frac{T_0}{m_X} \right)^n \int_{z_2}^{z_1} (1+z)^{n-1} dz, \end{aligned} \quad (5)$$

where $\dot{\rho}_{\text{ann}} = 2E_a \Gamma_a$ is the rate of energy injection by annihilations, $\rho_{\gamma 0}$ is the present energy density in the CMB, T_0 is the present CMB temperature, $n_{X0} \equiv n_X(z)(1+z)^{-3}$, and $t_\star \equiv 2.4 \times 10^{19}$ s. We have assumed the universe is radiation dominated (this assumption will be accurate enough at the redshifts relevant to our calculation) so that $t \approx 0.301 g_\star^{-1/2} m_{\text{Pl}} T^{-2} \equiv t_\star (1+z)^{-2}$, where m_{Pl} is the Planck mass, $g_\star = 3.36$ is the number of effectively massless degrees of freedom at $T \ll \text{MeV}$, and t_\star is fixed by the CMB temperature measured at $z = 0$. The result for $n = 0$ is

$$\frac{\delta\rho_\gamma}{\rho_\gamma} = A \ln \left(\frac{z_1}{z_2} \right), \quad (6)$$

and for $n = 1$

$$\frac{\delta\rho_\gamma}{\rho_\gamma} = A \frac{T_1 - T_2}{m_X}, \quad (7)$$

where

$$A \equiv \frac{4t_* E_a \sigma_0 n_{X0}^2}{\rho_{\gamma 0}}, \quad (8)$$

and $T_i \equiv T(z_i)$.

We use $z_1 = z_{\text{DC}}$ and $z_2 = z_C$ to find the chemical potential $\mu = 1.4\delta\rho_\gamma/\rho_\gamma$,¹ with the results

$$\begin{aligned} \mu = 5.1A = 2.9 \times 10^{-4} f \left(\frac{m_X}{\text{MeV}} \right)^{-1} \\ \times \left[\left(\frac{\sigma_0}{6 \times 10^{-27} \text{ cm}^3 \text{ s}^{-1}} \right) (\Omega_{X\bar{X}} h^2)^2 \right] \quad (\text{for } n=0), \end{aligned} \quad (9)$$

and

$$\begin{aligned} \mu = 2.0 \times 10^6 A \frac{T_0}{m_X} = 2.7 \times 10^{-8} f \left(\frac{m_X}{\text{MeV}} \right)^{-2} \\ \times \left[\left(\frac{\sigma_0}{6 \times 10^{-27} \text{ cm}^3 \text{ s}^{-1}} \right) (\Omega_{X\bar{X}} h^2)^2 \right] \quad (\text{for } n=1), \end{aligned} \quad (10)$$

where $\Omega_{X\bar{X}} h^2 = 94(m_X/\text{MeV})(n_{X0} + n_{\bar{X}0})/\text{cm}^{-3}$.

Observationally $|\mu| < 9 \times 10^{-5}$ [4] so, for $n=0$, we have the bound

$$f \left(\frac{m_X}{\text{MeV}} \right)^{-1} \left[\left(\frac{\sigma_0}{6 \times 10^{-27} \text{ cm}^3 \text{ s}^{-1}} \right) (\Omega_{X\bar{X}} h^2)^2 \right] < 0.3. \quad (11)$$

Similarly, for $n=1$ we find

$$f \left(\frac{m_X}{\text{MeV}} \right)^{-2} \left[\left(\frac{\sigma_0}{6 \times 10^{-27} \text{ cm}^3 \text{ s}^{-1}} \right) (\Omega_{X\bar{X}} h^2)^2 \right] < 3.3 \times 10^3. \quad (12)$$

We have chosen to scale the cross section as $(\sigma_0/6 \times 10^{-27} \text{ cm}^3 \text{ s}^{-1})$ because this is approximately the value at which a non-relativistic particle will have relic density $\Omega_{X\bar{X}} h^2 = 1$ if it freezes out as a result of its annihilations while in thermal equilibrium. The reader should keep in mind that Ω_X is not necessarily the contribution of X to the present energy density if, for example, the particle decays subsequent to distorting the CMB.

Note that the constraint for $n=1$ is roughly m_X/T_{DC} times weaker than the constraint for $n=0$, where T_{DC} is the temperature at z_{DC} . Constraints on $n=1$ particles that fall

¹This assumes a negligible increase in the number of photons, which is valid even in the case of an electromagnetic cascade (see Appendix A).

out of kinetic equilibrium at $T_K > T_{\text{DC}}$ can be roughly estimated from the given $n=1$ constraints by multiplying by a factor T_K/T_{DC} (see Ref. [24]).

The Compton- y distortion can be obtained by changing the limits of integration in Eq. (5) from z_{DC} and z_C to z_C and z_{rec} . For simplicity, we replace the lower limit z_{rec} by the redshift of matter-radiation equality, $z_{\text{eq}} \approx 2.5 \times 10^4 \Omega_0 h^2$ (where Ω_0 is the present density in matter), and we ignore deviations from $t \propto T^{-2}$. The precise value of this lower limit is not important (because of the log dependence) so we assume $z_{\text{eq}} = 3200$.

For $n=0$,

$$y \approx \frac{\mu}{1.4} \frac{1}{4} \frac{\ln(z_C/z_{\text{eq}})}{\ln(z_{\text{DC}}/z_C)} = 0.15\mu, \quad (13)$$

while the observational bound is $|y| < 1.5 \times 10^{-5}$ [4], giving a bound essentially identical to Eq. (11). For $n=1$, $y \approx 0.005 \mu$, so the bound will be significantly weaker than Eq. (12).

In the case of $n=0$, we predict that the μ and y distortions will always appear together, with the relationship $y \approx 0.15 \mu$. Fixsen *et al.* [4] do not give joint constraints on μ and y so we perform our own linear fit to the data in their Table 4, using the formula

$$\begin{aligned} I_0(\nu) - B_\nu(T_0) - G_0 g(\nu) \\ = \Delta T \frac{\partial B_\nu}{\partial T} + G_1 g(\nu) + 1.4 \frac{\delta\rho}{\rho} \left(\frac{\partial S_c}{\partial \mu} + 0.15 \frac{\partial S_c}{\partial y} \right), \end{aligned} \quad (14)$$

where $I_0(\nu) - B_\nu(T_0) - G_0 g(\nu)$ is taken from Ref. [4] (along with the necessary error bars), $g(\nu) = \nu^2 B_\nu(9 \text{ K})$ is the galactic contamination model used by [4], and $\partial S_c/\partial p$ is the deviation from a blackbody as parameter p is varied. We constrain jointly the parameters ΔT , G_1 , and $\delta\rho/\rho$. Based only on statistical errors, the 95% confidence upper bound on the energy injection is $\delta\rho/\rho < 1.6 \times 10^{-5}$. Our analysis is complicated by the significant systematic errors, 1×10^{-5} and 4×10^{-6} , quoted by [4] for μ and y , respectively. It is not clear how these should be combined with the statistical error, so we choose arbitrarily to add the two systematic errors linearly, and then add the result in quadrature to the statistical error, to find a final 95% confidence upper bound $\delta\rho/\rho < 4.1 \times 10^{-5}$. We finally obtain the bound

$$f \left(\frac{m_X}{\text{MeV}} \right)^{-1} \left[\left(\frac{\sigma_0}{6 \times 10^{-27} \text{ cm}^3 \text{ s}^{-1}} \right) (\Omega_{X\bar{X}} h^2)^2 \right] < 0.2. \quad (15)$$

The combined constraints are plotted as the solid lines in Fig. 1 (for $n=1$ we just use the μ constraint).

We truncated Fig. 1 at $m_X = 1 \text{ GeV}$, where hadronic interactions become important; however, the CMB bound should continue to apply at higher energies, as long as f is computed to account for non-interacting annihilation products. Even neutral annihilation products can contribute to the CMB distortion if they are coupled to the plasma in any way,

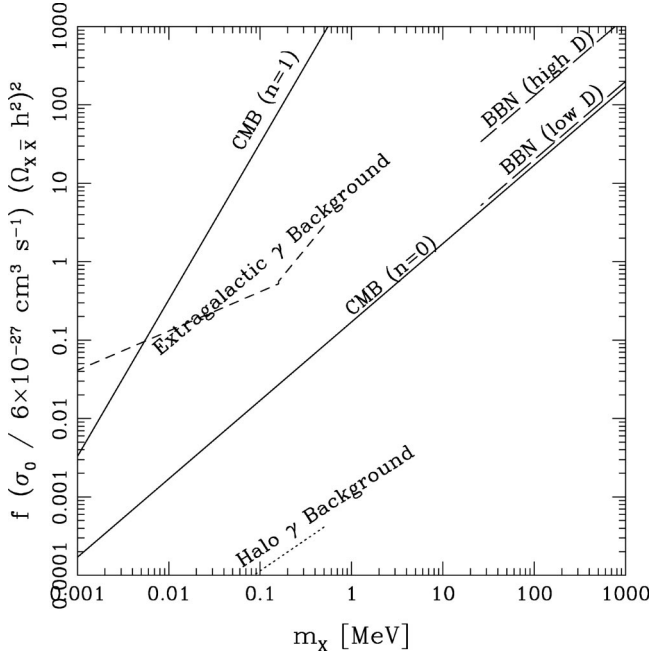


FIG. 1. Bounds on relic particles from residual annihilations. The space *above* the lines is ruled out in each case. Except for the upper solid line, all bounds are for particles with $\langle \sigma_a |v| \rangle = \sigma_0$ (i.e., $n=0$). The lower (upper) solid line is the constraint from the CMB (including both μ and y distortions) for $n=0$ ($n=1$). The upper (lower) long-dashed line is the constraint from BBN using the high (low) deuterium abundance (the low D constraint and the CMB constraint are practically identical but we have introduced a slight offset for clarity). The dashed line is the constraint from the diffuse photon background produced by extragalactic annihilations, and the dotted line is the constraint from the diffuse photon background produced by annihilations in the Milky Way halo. The BBN constraints apply for $m_X > 26$ MeV, the threshold for photodissociation of ${}^4\text{He}$ to D. For the CMB and BBN constraints, f is the fraction of the annihilation energy that interacts electromagnetically. For the photon background constraints, f should be replaced by f_γ , the fraction of annihilations that produce two photons with energy m_X (the lines for these constraints are terminated at the electron mass because $f_\gamma \ll f$ is likely if other annihilation channels are open). For the case of equivalent particle and antiparticle, substitute $\Omega_{X\bar{X}} \rightarrow \Omega_X$, and $\sigma_0/6 \times 10^{-27} \text{ cm}^3 \text{ s}^{-1} \rightarrow \sigma_0/3 \times 10^{-27} \text{ cm}^3 \text{ s}^{-1}$.

for example, if they heat the background protons through hadronic interactions (see Ref. [9,10] for discussions of hadronic interactions during this epoch). This is not generally true for the other constraints that we review in Sec. III.

These constraints apply to a particle that is distinct from its antiparticle; however, to convert to the case where particle and antiparticle are equivalent, it is only necessary to make the substitutions $\Omega_{X\bar{X}} \rightarrow \Omega_X$, and $\sigma_0/6 \times 10^{-27} \text{ cm}^3 \text{ s}^{-1} \rightarrow \sigma_0/3 \times 10^{-27} \text{ cm}^3 \text{ s}^{-1}$. The change in cross section normalization cancels the increase in the annihilation rate at fixed total contribution to the critical density (i.e., for the inequivalent case $\Gamma_a \propto n_X n_{\bar{X}} \propto \Omega_{X\bar{X}}^2/4$, but for the equivalent case $\Gamma_a \propto n_X^2/2 \propto \Omega_X^2/2$). The scale $3 \times 10^{-27} \text{ cm}^3 \text{ s}^{-1}$ for the cross section is natural also because it gives $\Omega_X h^2 \approx 1$. The same substitutions can be used to convert any of the constraints in Sec. III.

III. COMPARISON WITH OTHER CONSTRAINTS ON RESIDUAL ANNIHILATIONS

In this section we compute bounds, in a form similar to Eq. (11), from the production of deuterium by photodissociation of ${}^4\text{He}$ (Sec. III A), from the diffuse photon background produced by extragalactic annihilations at $z < z_{\text{rec}}$ (Sec. III B), and from the diffuse photon background produced by annihilations in our galaxy (Sec. III C). We restrict our attention to $n=0$ because the $n=1$ bound is very weak in all cases.

A. Photodissociation of ${}^4\text{He}$

At roughly the same time that the CMB energy spectrum becomes vulnerable to distortion by energy injection, primordial produced ${}^4\text{He}$ nuclei become vulnerable to photodissociation by high energy annihilation products. At earlier times the nuclei were protected from destruction because photons with high enough energy ($E_\gamma \gtrsim 20$ MeV) to destroy nuclei instead pair produce or elastic scatter on the CMB photons ($\gamma\gamma \rightarrow e^+e^-$, or $\gamma\gamma \rightarrow \gamma\gamma$). This shielding is effective for $E_\gamma \gtrsim m_e^2/44T$, where the numerical factor accounts for the fact that photons in the high energy tail of the CMB spectrum are still very numerous (see Ref. [25], and references therein, for a full discussion). Once $m_e^2/44T \gtrsim 20$ MeV, annihilation products can dissociate ${}^4\text{He}$, either directly, or indirectly through a cascade when $m_X \gtrsim m_e^2/44T$.

Bounds on energy injection can be derived by considering the ${}^3\text{He}$ or the D produced when ${}^4\text{He}$ nuclei are dissociated, and requiring that the amount created is not greater than the observationally inferred primordial abundances (bounds from direct photodissociation of deuterium extend to slightly lower annihilation energy but are significantly weaker [7]). Previous analyses [11,26] used ${}^3\text{He} + \text{D}$ because the upper limit on the primordial abundance of D was poorly known; however, there is considerable uncertainty in the post-big bang production and destruction of ${}^3\text{He}$ so we will use D because its abundance is now more robustly measured in QSO absorption systems [3], with a very conservative upper bound $n_D/n_H \equiv D/H < 3 \times 10^{-4}$ (high D) [27], or, more probably, $D/H < 4 \times 10^{-5}$ (low D) [28].

Protheroe, Stanev, and Berezhinsky [29] presented a detailed computation of the (redshift dependent) quantity of D produced for a given amount of injected energy, $N_D(z)$. With this input, the ratio D/H is given by

$$\frac{D}{H} = \int \frac{N_D(z) 2E_a \langle \sigma_a |v| \rangle n_X^2}{n_H} dt. \quad (16)$$

For $n=0$ this is

$$\begin{aligned} \frac{D}{H} &= 2E_a \int \frac{N_D(z) \sigma_0 n_{X0}^2 (1+z)^6}{n_{H0} (1+z)^3} \frac{2t_\star}{(1+z)^3} dz \\ &= \frac{4t_\star E_a \sigma_0 n_{X0}^2}{n_{H0}} \int N_D(z) dz = \frac{9800 t_\star E_a \sigma_0 n_{X0}^2}{n_{H0}}, \end{aligned} \quad (17)$$

where we have used the results in [29] and evaluated the integral numerically. The constraint on annihilations of particles with $m_X \gtrsim 26$ MeV (the energy needed to dissociate ${}^4\text{He}$ into D) is

$$f\omega_B^{-1} \left(\frac{m_X}{\text{MeV}} \right)^{-1} \left[\left(\frac{\sigma_0}{6 \times 10^{-27} \text{ cm}^3 \text{ s}^{-1}} \right) (\Omega_{X\bar{X}} h^2)^2 \right] < 1.3 \text{ (high D), or } < 0.2 \text{ (low D)}, \quad (18)$$

weaker than the CMB bound if the high deuterium abundance is used, but similar for the low deuterium abundance (recall $\omega_B = \Omega_B h^2 / 0.02 \approx 1$). These constraints are plotted as the long-dashed lines in Fig. 1.

This calculation is not exactly correct unless $m_X \gg 26$ MeV because our use of the results in [29] assumes that the annihilation products are energetic enough to produce a cascade. A more careful calculation would weaken the bound slightly for $m_X \sim 26$ MeV [11].

Our constraint appears to be several orders of magnitude stronger than the constraint described by Eq. (9) in Ref. [26]. They used the observational bound $({}^3\text{He} + D)/H \lesssim 1.1 \times 10^{-4}$, which, considering that ${}^3\text{He}$ is produced ~ 24 times more efficiently than D [29], should give a bound somewhat stronger than our Eq. (18). We believe that the discrepancy is the result of a numerical error in their calculation. Our result for the $({}^3\text{He} + D)/H$ calculation agrees with [11]; however, we do not use this result for our annihilation constraint because the deuterium constraint should be more reliable [3].

B. Extragalactic γ background

Recently, Kribs and Rothstein [30] used the observed γ -ray background to constrain late decaying particles. Gao, Stecker, and Cline [13] computed the expected γ -ray flux from annihilations of a possible lightest supersymmetric particle. Here we generalize this annihilation calculation to match the form of the constraint derived from the CMB. Unlike the previous constraints, the constraint we compute now only applies to annihilations directly to two photons, which typically will be sub-dominant for particles with mass greater than the electron mass (assuming particle X does not couple directly to photons). Therefore, we will only calculate the constraint for $m_X < 0.5$ MeV (constraints for general annihilation products would be strongly model dependent).

Temporarily ignoring the possibility that photons produced after recombination (at $z_{\text{rec}} \approx 1100$) are absorbed on their way to the observer, the observed energy flux at present from extragalactic annihilations to photons is

$$\frac{dJ}{dEd\Omega} = \frac{2c}{4\pi} \int_0^{z_{\text{rec}}} dt f_\gamma m_X \Gamma_a(z) \times \delta[E_o(1+z) - m_X] (1+z)^{-3}, \quad (19)$$

where f_γ is the fraction of annihilations that produce a pair of photons with $E_\gamma = m_X$. Using $dt/da = 3t_0 a^{1/2}/2 = H_0^{-1} a^{1/2}$ for an Einstein-de Sitter universe, and $\delta(E_o a^{-1} - m_X) = a^2 \delta(a - E_o/m_X) E_o^{-1}$, we find

$$\begin{aligned} \frac{dJ}{dEd\Omega} &= \frac{2c}{4\pi H_0} f_\gamma \sigma_0 n_{X0}^2 \left(\frac{m_X}{E_o} \right)^{3/2} \\ &\approx \frac{3.9 \times 10^{-4}}{\text{cm}^2 \text{ s sr}} f_\gamma \left(\frac{m_X}{\text{MeV}} \right)^{-2} \left(\frac{m_X}{E_o} \right)^{3/2} \\ &\quad \times \left[\left(\frac{\sigma_0}{6 \times 10^{-27} \text{ cm}^3 \text{ s}^{-1}} \right) \right. \\ &\quad \left. \times (\Omega_{X\bar{X}} h^2)^2 \right], \quad (20) \end{aligned}$$

where we have taken $n=0$. The photons we are considering, with energy $E_\gamma < 0.5$ MeV, will in fact lose most of their energy by Compton scattering if they are produced at $z \gtrsim 200$ (see Ref. [31]), so the maximum redshift factor is $m_X/E_o = 200$.

We derive a bound on annihilations by requiring that the predicted photon background is not greater than the observed one. After considering observations of the photon background at all relevant energies (see Ref. [32–34]), we find that the ASCA data in the energy range $0.8 \text{ KeV} \leq E_o \leq 2.5 \text{ KeV}$ provides the best constraint on the annihilating particles that we consider. The background in this range is conservatively bounded by $dJ/dEd\Omega < 0.36 (E_o/\text{MeV})^{-0.58} \text{ cm}^{-2} \text{ s}^{-1} \text{ sr}^{-1}$ [33].

For $160 \text{ KeV} \leq m_X < 500 \text{ KeV}$, the best constraint is derived from photons produced at $z \approx 200$. Setting $E_o = m_X/200$, we obtain the bound

$$f_\gamma \left(\frac{m_X}{\text{MeV}} \right)^{-1.42} \left[\left(\frac{\sigma_0}{6 \times 10^{-27} \text{ cm}^3 \text{ s}^{-1}} \right) (\Omega_{X\bar{X}} h^2)^2 \right] \leq 7.6. \quad (21)$$

The best bound for lower annihilation energies comes from observations at $E_o \approx 0.8 \text{ KeV}$:

$$f_\gamma \left(\frac{m_X}{\text{MeV}} \right)^{-1/2} \left[\left(\frac{\sigma_0}{6 \times 10^{-27} \text{ cm}^3 \text{ s}^{-1}} \right) (\Omega_{X\bar{X}} h^2)^2 \right] \leq 1.3. \quad (22)$$

Figure 1 shows these constraints as the dashed line.

C. Annihilations in the Milky Way halo

The observability of annihilations to photons in our own galaxy has been discussed in many papers, including [14–16]. In this subsection we combine the latest observational limits on the photon background with the calculation by Kamionkowski [35] and Jungman, Kamionkowski, and Griest [17] of the flux expected from halo annihilations to derive a bound in the form of Eq. (11). As discussed in the previous subsection, we only consider annihilations to two photons of particles with $m_X < 0.5$ MeV.

Jungman, Kamionkowski, and Griest [17] assume the model

$$\rho(r) = \rho_0 \frac{R^2 + a^2}{r^2 + a^2} \quad (23)$$

for the dark matter density distribution in the Galaxy, where R is the distance of the Sun from the galactic center, a is the core radius, and r is the distance from the center of the galaxy. Note that simulations of cold dark matter models predict central cusps instead of a core [36], which could lead to enhanced annihilation signals toward the center of the Galaxy; however, we want to be conservative so we do not assume a cusp. Re-writing Eq. (10.1) of Ref. [17] to include the possibility that the particle X does not make up all the dark matter, we find that the energy flux at $E_o = m_X$ is

$$\begin{aligned} \frac{dJ}{dEd\Omega} \approx & f_\gamma \frac{3.0}{\text{cm}^2 \text{ s sr}} \left(\frac{m_X}{\text{MeV}} \right)^{-2} \left(\frac{\rho_D^{0.4}}{\Omega_D h^2} \right)^2 I(\psi) \\ & \times \left[\left(\frac{\sigma_0}{6 \times 10^{-27} \text{ cm}^3 \text{ s}^{-1}} \right) (\Omega_{X\bar{X}} h^2)^2 \right], \quad (24) \end{aligned}$$

where $I(\psi) \sim 1$ depends on the observation angle ψ , $\Omega_D \geq \Omega_{X\bar{X}}$ is the contribution to the critical density from all kinds of dark matter, and $\rho_D^{0.4} \sim 1$ is the density of dark matter near the solar radius, in units of 0.4 GeV cm^{-3} . We have assumed $\rho_X(r) \propto \rho_D(r)$, and used the detector energy resolution, $\Delta E/E \sim 0.2$, appropriate for the energy bins in Fig. 10 of Ref. [32].

The relevant energy range for the halo annihilations we are considering, $1\text{--}500 \text{ KeV}$, corresponds to a ‘‘bump’’ in the observed spectrum (see [32]). To be conservative, we construct a simple bound by comparison with the single power law $dJ/dEd\Omega \leq 0.022(E_o/\text{MeV})^{-1.2} \text{ cm}^{-2} \text{ s}^{-1} \text{ sr}^{-1}$, which is an upper bound on the energy flux in the full range $1 \text{ KeV} \leq E_o \leq 100 \text{ GeV}$ [32]. Since annihilations to two photons produce a line source at $E_o = m_X$, we have the bound

$$\begin{aligned} f_\gamma \left(\frac{m_X}{\text{MeV}} \right)^{-0.8} (\Omega_D h^2)^{-2} \left[\left(\frac{\sigma_0}{6 \times 10^{-27} \text{ cm}^3 \text{ s}^{-1}} \right) \right. \\ \left. \times (\Omega_{X\bar{X}} h^2)^2 \right] < 0.008, \quad (25) \end{aligned}$$

which we show in Fig. 1 (the observationally favored value for the total mass density is $\Omega_D h^2 \approx 0.15$ [37,38], but we use 0.3 as a more conservative upper bound). For particles that survive to the present, this bound is generally stronger than the bound from distortions of the CMB. Note that our calculation is a somewhat rough estimate because the observational bounds are considerably lower at some energies than the power law we adopted [32], the energy bin width $\Delta E/E$ is approximate, and we used $I(\psi) = 1$ when its value can be higher for observation angles near the galactic center [17].

For particles with $m_X > 0.5 \text{ MeV}$ we might consider the observation of annihilation products other than photons (e.g., positrons); however, Ref. [17] concludes that these signals

cannot be used to conclusively rule out dark matter candidates because of astrophysical uncertainties.

IV. DISCUSSION

Some of the parameter space that can be constrained by residual annihilations is covered already by other kinds of constraints. To put the annihilation constraints in perspective we review the primary astrophysical ones.

BBN gives limits on the expansion rate of the universe at $T \sim 1 \text{ MeV}$ (sometimes described as a limit on the effective number of light neutrinos, e.g., Ref. [3]). The expansion rate would be affected by an additional particle with mass in the range where our CMB bound is most constraining ($m_X \lesssim \text{MeV}$), if the particle’s number density at the time of BBN is equal to the thermal equilibrium value. Therefore, the annihilation bound on particles with $m_X \lesssim \text{MeV}$ is only nonredundant for particles that were not in thermal equilibrium at the time of nucleosynthesis.

Particles with $m_X \geq 5 \text{ MeV}$ are only constrained by our bound if their density, extrapolated by $(1+z)^{-3}$ from the time they influence the CMB to the present, is substantially greater than the present critical density, or if their cross section is very large but their number density is somehow higher than the density obtained from freeze-out of their annihilations (see Fig. 1). The first case would require that the particle decays invisibly or otherwise disappears between $z \sim 10^6$ and the present, and the second requires that the particle was formed by decays of a heavier particle (or some other mechanism) after the freeze-out temperature for its annihilations.

New particles that can be created in stars (e.g., by plasmon decay, $\gamma \rightarrow X\bar{X}$) are constrained by their action as additional sources of cooling. Constraints from observations of globular cluster stars apply for $m_X \lesssim 10 \text{ keV}$ [2]. Similarly, cooling in supernovae, specifically SN 1987A, can be influenced by the creation of new particles with mass $m_X \lesssim 30 \text{ MeV}$; however, these constraints depend on the details of the particle interactions in the plasma (e.g., Ref. [39]).

In summary, the bound from distortions of the CMB energy spectrum probably cannot be a useful constraint on annihilations of light ($m_X \lesssim 0.5 \text{ MeV}$) dark matter particles (e.g., warm dark matter) to photons, because the bound from annihilations in our Galaxy is always stronger. It is most interesting as a constraint on *dark matter* particles in the mass range $0.5 \lesssim m_X \lesssim 5 \text{ MeV}$, and *any* particle that decays invisibly between $z \approx 10^6$ and the present, although in either case the particle must also evade the bound from the expansion rate of the universe during BBN. Finally, although we have not discussed in this paper the case of annihilations of particles with cross sections that increase with decreasing temperature (e.g., [40]), it seems likely that they can be very tightly constrained by the kinds of tests we have discussed.

ACKNOWLEDGMENTS

R.J.S. and T.P.W. were supported by the Department of Energy (DE-FG02-91ER40690).

APPENDIX

The number density of photons in an electromagnetic cascade formally diverges at low energy, because the distribution of photons is given by $dn/dE_\gamma \propto E_\gamma^{-1.5}$ (see [25], and references therein). In this appendix, we show that the number of injected photons is still effectively negligible for our purpose of calculating the chemical potential for the Bose-Einstein distortion, because very low energy photons, i.e., frequency less than $x_{c,DC} \approx 3.0 \times 10^{-6} z^{1/2}$, are absorbed through the inverse-double Compton process before they can be scattered up in energy [6].

We determine the mean energy per injected photon by integrating the energy distribution from $E_{\text{cut}} = x_{c,DC} T$ to $E_{\text{max}}/2 = m_e^2/(22T)$, the energy at which the power law index changes from -1.5 to -5 (for simplicity, we ignore the contribution from $E_\gamma > E_{\text{max}}/2$). The normalization of the distribution is found by computing the total energy in the cascade:

$$E \propto \int_0^{E_{\text{max}}/2} E_\gamma^{-0.5} dE_\gamma = 2 \left(\frac{E_{\text{max}}}{2} \right)^{1/2}, \quad (\text{A1})$$

yielding $dn/dE_\gamma = E(2E_{\text{max}})^{-1/2} E_\gamma^{-1.5}$. Then the total number of photons is

$$N = \int_{E_{\text{cut}}}^{E_{\text{max}}/2} \frac{dn}{dE_\gamma} dE_\gamma = 2E(2E_{\text{max}}E_{\text{cut}})^{-1/2}, \quad (\text{A2})$$

and the mean photon energy is

$$\begin{aligned} \frac{E}{N} &= \left(\frac{E_{\text{max}}E_{\text{cut}}}{2} \right)^{1/2} = \left(\frac{m_e^2 x_{c,DC}}{44} \right)^{1/2} \\ &= 0.13 z^{1/4} \text{ KeV}. \end{aligned} \quad (\text{A3})$$

If small changes in the number density are present, the chemical potential is (see [6])

$$\begin{aligned} \mu &= \frac{1}{2.143} \left(3 \frac{\delta \rho_\gamma}{\rho_\gamma} - 4 \frac{\delta n_\gamma}{n_\gamma} \right) \\ &= 1.4 \frac{\delta \rho_\gamma}{\rho_\gamma} \left(1 - \frac{3.6T}{E/N} \right), \end{aligned} \quad (\text{A4})$$

where we have used $\rho_\gamma/n_\gamma = 2.7T$ for a blackbody. From Eqs. (A3) and (A4) we see that, at $z = 10^6$, including the effect of injected photons decreases μ to 0.8 times the value it would have without them, and the change becomes even smaller at lower redshift.

-
- [1] D.E. Groom *et al.*, *Eur. Phys. J. C* **15**, 1 (1998).
 [2] G.G. Raffelt, *Annu. Rev. Nucl. Part. Sci.* **49**, 163 (1999).
 [3] K.A. Olive, G. Steigman, and T.P. Walker, *Phys. Rep.* **333**, 389 (2000).
 [4] D.J. Fixsen, E.S. Cheng, J.M. Gales, R.A. Shafer, and E.L. Wright, *Astrophys. J.* **473**, 576 (1996).
 [5] C. Burigana, G. De Zotti, and L. Danese, *Astrophys. J.* **379**, 1 (1991).
 [6] W. Hu and J. Silk, *Phys. Rev. D* **48**, 485 (1993).
 [7] J. Ellis, G.B. Gelmini, J.P. Lopez, D.V. Nanopoulos, and S. Sarkar, *Nucl. Phys.* **B373**, 399 (1992).
 [8] B.W. Lee and S. Weinberg, *Phys. Rev. Lett.* **39**, 165 (1977).
 [9] M.H. Reno and D. Seckel, *Phys. Rev. D* **37**, 3441 (1988).
 [10] J.S. Hagelin, R.J.D. Parker, and A. Hankey, *Phys. Lett. B* **215**, 397 (1988).
 [11] J.A. Frieman, E.W. Kolb, and M.S. Turner, *Phys. Rev. D* **41**, 3080 (1990).
 [12] D.B. Cline and Y. Gao, *Astron. Astrophys.* **231**, L23 (1990).
 [13] Y. Gao, F.W. Stecker, and D.B. Cline, *Astron. Astrophys.* **249**, 1 (1991).
 [14] L. Bergstrom and H. Snellman, *Phys. Rev. D* **37**, 3737 (1988).
 [15] S. Rudaz, *Phys. Rev. D* **39**, 3549 (1989).
 [16] S. Rudaz and F.W. Stecker, *Astrophys. J.* **368**, 406 (1991).
 [17] G. Jungman, M. Kamionkowski, and K. Griest, *Phys. Rep.* **267**, 195 (1996).
 [18] J. Bernstein and S. Dodelson, *Phys. Rev. D* **41**, 354 (1990).
 [19] R.A. Sunyaev and Ya.B. Zeldovich, *Annu. Rev. Astron. Astrophys.* **18**, 537 (1980).
 [20] W. Hu and J. Silk, *Phys. Rev. Lett.* **70**, 2661 (1993).
 [21] R.J. Scherrer and M.S. Turner, *Phys. Rev. D* **33**, 1585 (1986).
 [22] R.J. Scherrer and M.S. Turner, *Phys. Rev. D* **34**, 3263(E) (1986).
 [23] H. Goldberg, *Phys. Rev. Lett.* **50**, 1419 (1983).
 [24] S. Hannestad, *Phys. Lett. B* **452**, 23 (1999).
 [25] S. Sarkar, *Rep. Prog. Phys.* **59**, 1493 (1996).
 [26] E.W. Kolb and A. Riotto, *Phys. Rev. D* **54**, 3722 (1996).
 [27] J.K. Webb, R.F. Carswell, K.M. Lanzetta, R. Ferlet, M. Lemoine, A. Vidal-Madjar, and D.V. Bowen, *Nature (London)* **388**, 250 (1997).
 [28] S. Burles and D. Tytler, *Astrophys. J.* **507**, 732 (1998).
 [29] R.J. Protheroe, T. Stanev, and V.S. Berezinsky, *Phys. Rev. D* **51**, 4134 (1995).
 [30] G.D. Kribs and I.Z. Rothstein, *Phys. Rev. D* **55**, 4435 (1997).
 [31] A.A. Zdziarski and R. Svensson, *Astrophys. J.* **344**, 551 (1989).
 [32] P. Skreekumar *et al.*, *Astrophys. J.* **494**, 523 (1998).
 [33] L.-W. Chen, A.C. Fabian, and K.C. Gendreau, *Mon. Not. R. Astron. Soc.* **285**, 449 (1997).
 [34] E.W. Kolb and M.S. Turner, *The Early Universe* (Addison-Wesley, Reading, MA, 1990), p. 143.
 [35] M. Kamionkowski, astro-ph/9404079 (1994).
 [36] J.F. Navarro, C.S. Frenk, and S.D.M. White, *Astrophys. J.* **490**, 493 (1997).
 [37] J.R. Mould *et al.*, *Astrophys. J.* **529**, 786 (2000).
 [38] M. Donahue and G.M. Voit, *Astrophys. J. Lett.* **523**, 137 (1999).
 [39] S. Davidson, S. Hannestad, and G. Raffelt, *J. High Energy Phys.* **5**, 3 (2000).
 [40] J.G. Bartlett and L.J. Hall, *Phys. Rev. Lett.* **66**, 541 (1991).